International Conference on "Recent Trends in Technology and its Impact on Economy of India"
Guru Nanak College for Girls, Sri Mukstar Sahib, Punjab (India) (ICRTTIEI-17)
24th October 2017, www.conferenceworld.in ISBN: 978-93-86171-74-0

Plasmon Assisted and Visible Light Irradiated Efficient Organic Pollutants Degradation

Dinesh Kumar,[1] Chan Hee Park[2],Cheol Sang Kim[3]

[1,2,3]*Department of Bionanosystem Engineering, Chonbuk National University, Jeonju, South Korea*

ABSTRACT

Here, we have highlighted the preparation of plasmonic gold nanoparticles with three different morphologies i.e. nanospheres (AuNS), nanorods (AuNR), and nanostars (AuST)) and their application for light induced photo-degradation of organic pollutants like methylene blue, methyl orange and methyl red. Xe lamp has been used as a source of visible light (370-770 nm) for organic dyes degradation. Simple solution-based synthetic strategies have been used for the preparation of colloidally stable gold nanoparticles of 30-35 nm size with different structure. The hot electron/hole generation, which is excited plasmon with higher energy than fermi-level after light absorption in the nanostructures and LSPR excitation, are useful to increase the catalytic activity of plasmonic nanomaterials efficiently. AuNS, AuST and AuNR have shown more than 90% of dyes degradation efficiency in visible light. AuST shown better efficiency as compared to AuNS and AuNR, and took lesser reaction time for dyes degradation in visible light irradiation.

I. INTRODUCTION

In recent years, photo-catalysis processes using sunlight has been attracting great attention due to increasing environmental and energy related issues [1, 2]. Titanium dioxide (TiO_2) has proven to be the most commonly used photo-catalyst in applications such as environmental cleaning (organic dye degradation) and hydrogen energy generation [3, 4]. However, because of its wide band gap, TiO_2 limits its photo-absorption to the ultra-violet region only which contains about 5% of total sunlight. In order to extend the photo-response from the ultra-violet region to the visible light region, plasmonic nanoparticles could be an attractive alternative.

The plasmonic nanomaterials, especially gold nanoparticles, have strong light (visible and NIR) absorption and subsequent hot electron/hole generation capabilities due to localized surface plasmon resonance through non-radiative decay [5]. Hot electrons/holes have been employed for several types of plasmon-enhanced photo-catalytic and energy conversion processes like water splitting, dissociation of small molecules, or generation of photocurrent in photovoltaic devices [5-8]. In case of organic dyes photo-degradation, the electron transfer step plays a vital role. The electron transfer in turn depends on the potential difference, as the large redox potential difference between the donor and acceptor can hinder the passage of electrons [9, 10]. The plasmonic nanomaterials such as silver, gold or platinum nanoparticles has an intermediate redox potential value which helps in the electron transfer and therefore acts as an electron transport system [11]. Also, photo-catalytic efficeincy of metal nanoparticles increases with the changes in the shape (with increasing surface to volume ratio) and size (with decreasing size) [12].

In present report, we have highlighted the preparation of plasmonic gold nanoparticles (30-35 nm size) with

ISBN: 978-93-86171-74-0

three different morphologies i.e. nanospheres (AuNS), nanorods (AuNR), and nanostars (AuST)) using solution based synthesis methods and their application for light induced photo-degradation of organic pollutants like methylene blue, methyl orange and methyl red.

II. EXPERIMENTAL SECTION

Materials and methods. All chemical reagents were purchased from Sigma-Aldrich (St. Louis, MO, USA) and used as received without further purification. Transmission electron microscopy (TEM, H-7650, Hitachi, Japan) was used for the nanoparticles analysis. Extinction spectra were obtained with a UV spectrometer (SCINCO, South Korea). Structural analyses were performed using X-ray diffraction (Rigaku D/MAX 2500Tokyo, Japan). A Xe lamp (Ceramaxs, Waltham, USA) with a power density of 5.7 W/cm^2 was used as a visible light (390–770 nm) source.

Preparation of AuSTs. The synthesis of AuSTs (λ_{max} = 615 nm) was carried out by following previously reported solution based method [13]. In a typical experiment, 10 mL of HEPES (100 mM) solution was mixed with 15 mL of distilled water, followed by the addition of $HAuCl_4$ (500 µL, 20 mM) solution. The resulting reaction mixture was kept undisturbed for 30 min at 30 °C, the color of solution changed from light yellow to greenish blue.

Preparation of sodium citrate modified AuNSs. The spherical AuNSs (λ_{max} = 525 nm) were synthesized by using sodium citrate based method [14, 15]. In a boiling solution of HAuCl4 (0.5mM, 50 mL), 1.1 mL of sodium citrate (38 mM) was added under continuous stirring. The resulting reaction mixture was stirred vigorously for 20 min to reduce gold completely as the color turned from light yellow to wine red. After that the final reaction mixture was centrifuged 2 times at 9000 rpm and re-dispersed in distilled water for further use.

Preparation of CTAB modified AuNRs. Cetyltrimethyl ammonium bromide (CTAB) mediated seed growth method was used to prepare AuNRs (λ_{max} = 736 nm) [16]. To make seed solution, 0.01 M of $HAuCl_4$ solution (0.25 mL) was mixed with an aqueous solution of CTAB (9.75 mL, 0.1 M). The solution mixture color changed from light yellow to pale-brown while 600 µL of ice-cold solution of $NaBH_4$ (0.01 M) was quickly added with vigorous stirring. Then the seed solution was stored in a water bath for 3 h at room temperature (28 °C). In the next step, growth solution was prepared by mixing 475 mL of CTAB (0.1 M) with 20 mL of $HAuCl_4$ (0.01 M), 3.0 mL of $AgNO_3$ (0.01 M), and 3.2 mL of ascorbic acid (0.1 M) in slow stirring. The light yellow colored solution became colorless with the addition of ascorbic acid. In the last step, 3.8 mL of seed solution was quickly mixed with growth solution and shake little, and then the resulting reaction mixture was kept undisturbed for 12 h in a water bath at 28 °C.

Organic dyes degradation. A 10 mg/L of organic dye (Methylene blue or methyl red or methyl orange) was mixed with nanoparticles (0.1 mg/mL) and stirred for 30 min in dark to achieve adsorption-desorption equilibrium. In a typical dye photo-degradation reaction, 10 mL mixture of organic dye with nanoparticles was placed in a pyrex glass reactor and illuminated with visible light until the complete degradation. Samples have been taken out after every 10 min from the reaction mixture and nanoparticles were removed by centrifugation. Then, in order to monitor the rate of degradation reaction, the centrifuged samples were analyzed with UV-visible spectrophotometer. The effect of reducing agent ($NaBH_4$) on the rate of dye degradation was also

ISBN: 978-93-86171-74-0

analyzed by adding 50 µL of $NaBH_4$ (0.1 M). The reaction rate constant k for organic dye photo-degradation was calculated from the equation $-\ln(C/C_0) = kt$, where k is the rate constant (min^{-1}), and C_0 and C are the initial and final concentration of the dye molecule at time t.

III. RESULTS AND DISCUSSION

Analysis of various gold nanostructures

The TEM images (Figure 1A-C) shows a successful preparation of AuSTs, AuNSs, and AuNRs. AuSTs, AuNSs, and AuNRs showed plasmon resonance band at 615 nm, 525 nm, and 736 nm, respectively (Figure 1D-F). On the other hand, the structural analysis has been performed using X-ray diffraction (XRD) analysis. XRD spectra showed the peaks at 37.88°, 44.11°, 64.15° and 77.12° corresponding to (111), (200), (220) and (311) planes of the Au face-centred cubic (fcc) crystal structure [16, 17], respectively (Fig. 1G-I).

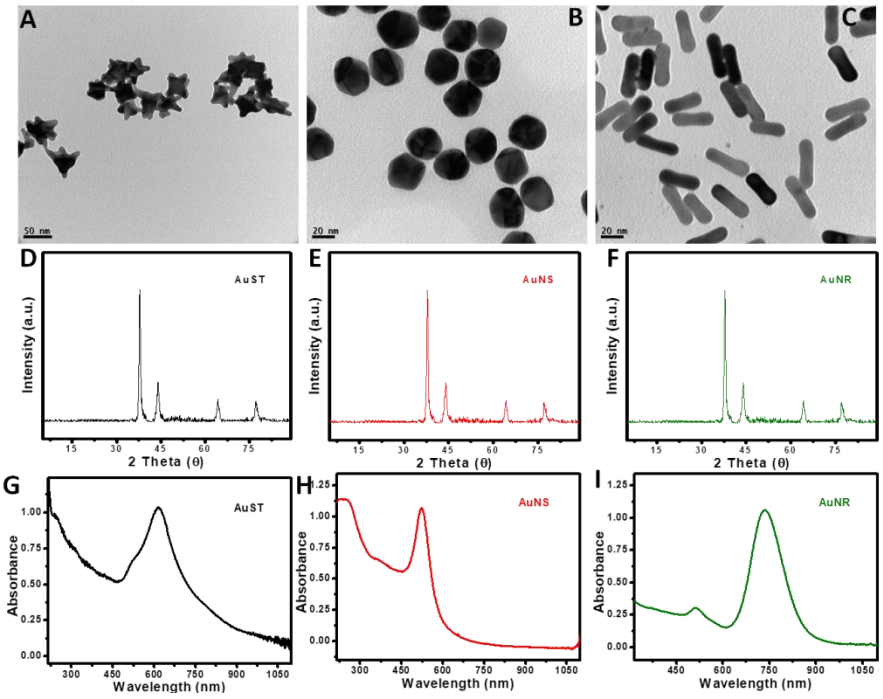

Figure 1 Synthesis and characterization of nanoparticles. (A, B, and C) TEM images of AuSTs, AuNSs, and AuNRs, respectively. (**D, E, and F**) UV-Visible spectrum, and (**G, H, and I**) XRD spectrum of AuSTs, AuNSs, and AuNRs, respectively.

Organic degradation

The photo-catalytic performance of gold nanostructures for the degradation of three organic dyes viz., methylene blue (MB), methyl red (MR) and methyl orange (MO) was observed in visible light irradiation. The progress of reaction was monitored by observing the change in absorption maxima (λ_{max}) of organic dyes using UV-Visible spectrophotometer. AuSTs, AuNSs and AuNRs took 75 min, 90 min and 120 min for complete degradation of MB, respectively (Fig. 2A-C). Whereas 110 min, 120 min and 150 min for complete degradation of MR and MO while using AuSTs, AuNSs and AuNRs under visible light illumination, respectively (Fig. 2D-I).

ISBN: 978-93-86171-74-0

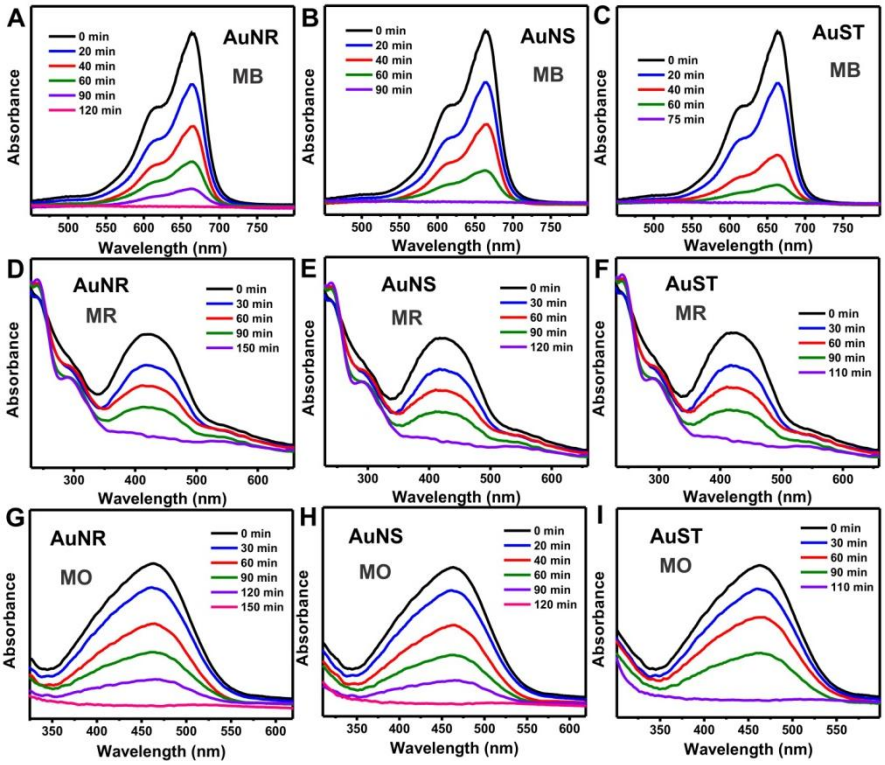

Figure 2. AuSTs, AuNSs, and AuNRs mediated time-dependent **(G)** methylene blue, **(H)** methyl red and **(I)** methyl orange degradation in the visible light illumination.

The results indicated that AuSTs, AuNSs and AuNRs degraded MB with 98.18%, 85.56% and 60.35%, MR with 98.2%, 84.77% and 60.48% and MO with 98.12%, 84.15% and 59.92% conversion efficiency in visible light irradiation for 75 min, and 110 min (Fig. 3D-F), respectively. For complete degradation of MB, MR and MO AuSTs took 75 min and 110 min (for MR and MO) with 0.084, 0.055 and 0.054 min^{-1} pseudo first order rate constant [18, 19] values (Fig. 3A-C), respectively, and has shown higher photocatalytic efficiency as compared to AuNSs and AuNRs. The broad plasmon resonance band of AuSTs and high surface to volume ratio might be the reasons for higher activity.

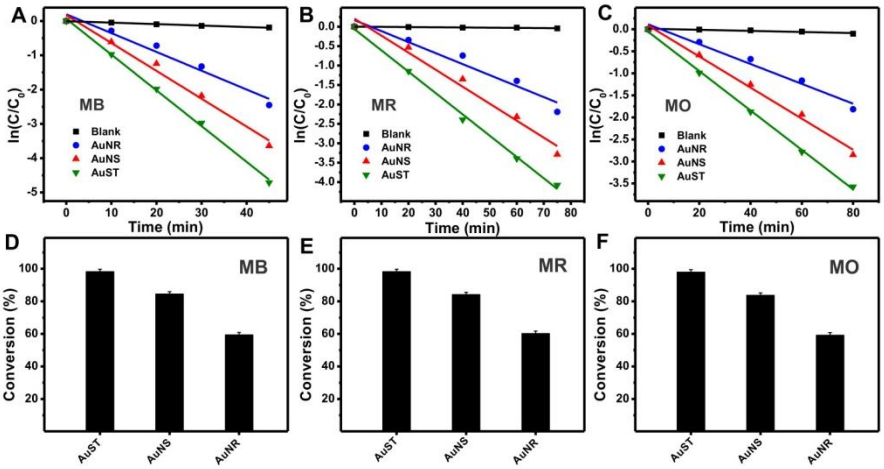

Figure 3. Effect of different gold nanoparticles on the rate of reaction for the degradation of **(A)** methylene blue,

ISBN: 978-93-86171-74-0

(B) methyl red and **(C)** methyl orange. Effect of different nanoparticles on the conversion efficiency of the visible light illuminated degradation of **(D)** methylene blue, **(E)** methyl red and **(F)** methyl orange.

The effect of reducing agent ($NaBH_4$) on AuSTs mediated MB, MR and MO complete degradation has also been analyzed by adding 50 µL of 0.1 M $NaBH_4$ to 10 mL of reaction mixture contains dye. All the three dye molecules were degraded completely in 20 min of reaction time while illuminated with visible light (Figure 4A-C). The dye degradation reaction in the prersence of $NaBH_4$ without nanoparticles shows incomplete complete efficiency even after 60 min of reaction time as shown in Figure 4D-F.

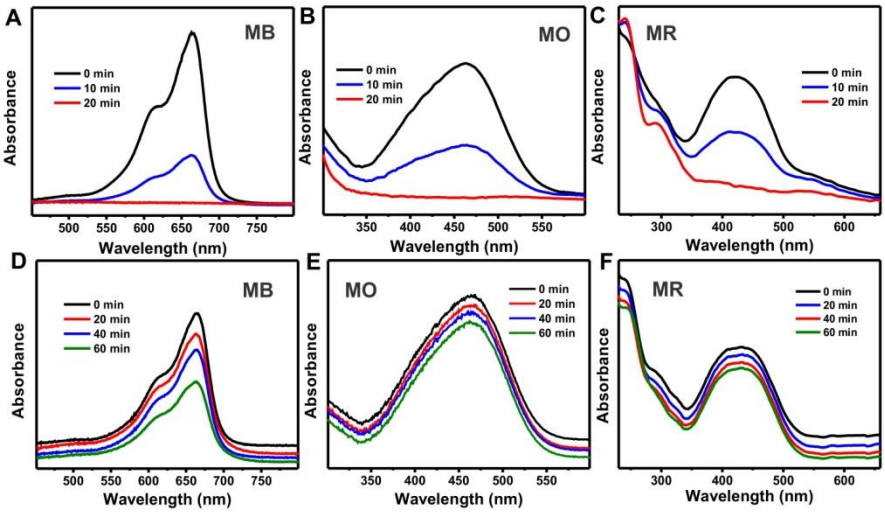

Figure 4. AuNSs mediated **(A)** methylene blue, **(B)** methyl orange, and **(C)** methyl red degradation in the presence of reducing agent ($NaBH_4$) under visible light illumination. **(D)** methylene blue, **(E)** methyl orange and **(F)** methyl red degradation in the presence of reducing agent ($NaBH_4$) only (without nanoparticles).

IV. CONCLUSIONS

In conclusion, in this report we have synthesized gold nanostructures (nanostars, nanospheres and nanorods) with uniform shape and size in three different morphologies utilizing solution based methods. The particle size of all three nanostructures was found to be 30-35 nm. All the prepared nanoparticles were used for three different organic dyes degradation in visible light irradiation. Gold nanostars took 75 min for complete degradation of MB, and 110 min for complete degradation of MR and MO. On the other hand, AuNSs took 90 min for complete degradation of MB, and 120 min for complete degradation of MR and MO. Whereas, AuNRs took 120 min for complete degradation of MB, and 150 min for complete degradation of MR and MO. AuSTs showed higher efficiency as compared to AuNSs and AuNRs with the pseudo first order rate 0.084, 0.055 and 0.054 min^{-1} for MB, MR, and MO, respectively. All the three dye molecules were degraded completely in 20 min of reaction time in the presence of $NaBH_4$ while illuminated with visible light using AuSTs.

V. ACKNOWLEDGEMENTS

This work was supported by the National Research Foundation of Korea (NRF-2016R1D1A1B03934226) Project. We are thankful to Center for University Wide Research Facility (CURF), Chonbuk National

ISBN: 978-93-86171-74-0

University, Jeonju, South Korea for TEM, and XRD analysis.

REFERENCES

[1] A. Paracchino, V. Laporte, K. Sivula, M. Grätzel, E. Thimsen, Highly active oxide photocathode for photoelectrochemical water reduction, Nat Mater, 10 (2011) 456-461.

[2] Q. Xiang, J. Yu, M. Jaroniec, Synergetic Effect of MoS2 and Graphene as Cocatalysts for Enhanced Photocatalytic H2 Production Activity of TiO2 Nanoparticles, Journal of the American Chemical Society, 134 (2012) 6575-6578.

[3] M.R. Hoffmann, S.T. Martin, W. Choi, D.W. Bahnemann, Environmental Applications of Semiconductor Photocatalysis, Chemical Reviews, 95 (1995) 69-96.

[4] H. Xu, S. Ouyang, L. Liu, P. Reunchan, N. Umezawa, J. Ye, Recent advances in TiO2-based photocatalysis, Journal of Materials Chemistry A, 2 (2014) 12642-12661.

[5] C. Clavero, Plasmon-induced hot-electron generation at nanoparticle/metal-oxide interfaces for photovoltaic and photocatalytic devices, Nat Photon, 8 (2014) 95-103.

[6] D. Kumar, S. Kaur, D.-K. Lim, Plasmon-assisted and visible-light induced graphene oxide reduction and efficient fluorescence quenching, Chemical Communications, 50 (2014) 13481-13484.

[7] D. Kumar, A. Lee, T. Lee, M. Lim, D.-K. Lim, Ultrafast and Efficient Transport of Hot Plasmonic Electrons by Graphene for Pt Free, Highly Efficient Visible-Light Responsive Photocatalyst, Nano Letters, 16 (2016) 1760-1767.

[8] S. Mubeen, J. Lee, N. Singh, S. Kramer, G.D. Stucky, M. Moskovits, An autonomous photosynthetic device in which all charge carriers derive from surface plasmons, Nat Nano, 8 (2013) 247-251.

[9] Z. Bian, T. Tachikawa, P. Zhang, M. Fujitsuka, T. Majima, Au/TiO2 Superstructure-Based Plasmonic Photocatalysts Exhibiting Efficient Charge Separation and Unprecedented Activity, Journal of the American Chemical Society, 136 (2014) 458-465.

[10] D. Ding, K. Liu, S. He, C. Gao, Y. Yin, Ligand-Exchange Assisted Formation of Au/TiO2 Schottky Contact for Visible-Light Photocatalysis, Nano Letters, 14 (2014) 6731-6736.

[11] L. Du, A. Furube, K. Yamamoto, K. Hara, R. Katoh, M. Tachiya, Plasmon-Induced Charge Separation and Recombination Dynamics in Gold−TiO2 Nanoparticle Systems: Dependence on TiO2 Particle Size, The Journal of Physical Chemistry C, 113 (2009) 6454-6462.

[12] K. Qian, B.C. Sweeny, A.C. Johnston-Peck, W. Niu, J.O. Graham, J.S. DuChene, J. Qiu, Y.-C. Wang, M.H. Engelhard, D. Su, E.A. Stach, W.D. Wei, Surface Plasmon-Driven Water Reduction: Gold Nanoparticle Size Matters, Journal of the American Chemical Society, 136 (2014) 9842-9845.

[13] J. Xie, J.Y. Lee, D.I.C. Wang, Seedless, Surfactantless, High-Yield Synthesis of Branched Gold Nanocrystals in HEPES Buffer Solution, Chemistry of Materials, 19 (2007) 2823-2830.

[14] N.G. Bastús, J. Comenge, V. Puntes, Kinetically Controlled Seeded Growth Synthesis of Citrate-Stabilized Gold Nanoparticles of up to 200 nm: Size Focusing versus Ostwald Ripening, Langmuir, 27 (2011) 11098-11105.

[15] F. Pincella, K. Isozaki, K. Miki, A visible light-driven plasmonic photocatalyst, Light Sci Appl, 3 (2014)

ISBN: 978-93-86171-74-0

e133.

[16] Z. Ban, Y.A. Barnakov, F. Li, V.O. Golub, C.J. O'Connor, The synthesis of core-shell iron@gold nanoparticles and their characterization, Journal of Materials Chemistry, 15 (2005) 4660-4662.

[17] Y. Lu, W. Chen, Sub-nanometre sized metal clusters: from synthetic challenges to the unique property discoveries, Chemical Society Reviews, 41 (2012) 3594-3623.

[18] X. Pan, Y.-J. Xu, Fast and spontaneous reduction of gold ions over oxygen-vacancy-rich TiO2: A novel strategy to design defect-based composite photocatalyst, Applied Catalysis A: General, 459 (2013) 34-40.

[19] Y.-J. Xu, Y. Zhuang, X. Fu, New Insight for Enhanced Photocatalytic Activity of TiO2 by Doping Carbon Nanotubes: A Case Study on Degradation of Benzene and Methyl Orange, The Journal of Physical Chemistry C, 114 (2010) 2669-2676.